Oxidized alkyl phospholipids stimulate sodium transport in proximal tubules *via* a nongenomic PPARγ-dependent pathway

Tomohito Mizuno[1], Nobuhiko Satoh[1], Shoko Horita[1], Hiroyuki Tsukada[1], Mayuko Takagi[1], Yusuke Sato[2], Haruki Kume[2], Masaomi Nangaku[1], and Motonobu Nakamura[1,*]

From the [1]Division of Nephrology and Endocrinology, and [2]Department of Urology, The University of Tokyo, Tokyo, Japan

Edited by Dennis Voelker

Oxidized phospholipids have been shown to exhibit pleiotropic effects in numerous biological contexts. For example, 1-O-hexadecyl-2-azelaoyl-sn-glycero-3-phosphocholine (azPC), an oxidized phospholipid formed from alkyl phosphatidylcholines, is a peroxisome proliferator–activated receptor gamma (PPARγ) nuclear receptor agonist. Although it has been reported that PPARγ agonists including thiazolidinediones can induce plasma volume expansion by enhancing renal sodium and water retention, the role of azPC in renal transport functions is unknown. In the present study, we investigated the effect of azPC on renal proximal tubule (PT) transport using isolated PTs and kidney cortex tissues and also investigated the effect of azPC on renal sodium handling *in vivo*. We showed using a microperfusion technique that azPC rapidly stimulated Na^+/HCO_3^- cotransporter 1 (NBCe1) and luminal Na^+/H^+ exchanger (NHE) activities in a dose-dependent manner at submicromolar concentrations in isolated PTs from rats and humans. The rapid effects (within a few minutes) suggest that azPC activates NBCe1 and NHE *via* nongenomic signaling. The stimulatory effects were completely blocked by specific PPARγ antagonist GW9662, ERK kinase inhibitor PD98059, and CD36 inhibitor sulfosuccinimidyl oleate. Treatment with an siRNA against PPAR gamma completely blocked the stimulation of both NBCe1 and NHE by azPC. Moreover, azPC induced ERK phosphorylation in rat and human kidney cortex tissues, which were completely suppressed by GW9662 and PD98059 treatments. These results suggest that azPC stimulates renal PT sodium-coupled bicarbonate transport *via* a CD36/PPARγ/mitogen-activated protein/ERK kinase/ERK pathway. We conclude that the stimulatory effects of azPC on PT transport may be partially involved in volume expansion.

Hypertension can lead to the development and progression of atherosclerosis, and it also contributes to the development of cardiovascular diseases (1). In contrast, atherosclerosis is known to be a risk factor for hypertension (2). However, the underlying mechanism for the development of hypertension because of atherosclerosis has not been elucidated yet. A large number of studies have demonstrated the role of oxidation products in the progression of atherosclerosis (3, 4). Because of oxidative stress, oxidized phospholipids (oxPLs) are generated from a variety of phospholipids containing polyunsaturated fatty acids (3). OxPLs are mainly accumulated in atherosclerotic lesions (5), and they are associated with endothelial dysfunction (3, 6), adhesion, transmigration, cytokine production by macrophages (5, 7), proliferation, migration, and phenotypic switching of vascular smooth muscle cells (8–10), and apoptosis (7). Although oxPLs exert both proatherogenic and protective effects by affecting diverse gene expression and signaling pathways, their proatherogenic action is predominant at the sites of tissue deposition of oxPLs, leading to the progression of atherosclerosis (5, 11, 12).

An increase in renal proximal tubule (PT) sodium reabsorption can lead to hypertension (13). Approximately 50 to 60% filtered Na^+ and 80% filtered HCO_3^- are reabsorbed from PT by the cooperative action of Na^+/H^+ exchanger 3 (NHE3) and vacuolar-type H^+-ATPase (V-ATPase) expressed on the luminal membranes and Na^+/HCO_3^- cotransporter 1 (NBCe1) expressed on the basolateral membranes (14–16). The functions of NHE3 and NBCe1 are regulated by humoral factors and various signaling mechanisms (14, 17). Indeed, we have previously reported some NHE3 and NBCe1 stimulators, such as angiotensin II (Ang II), insulin, and thiazolidinediones (TZDs) (18–22).

Peroxisome proliferator–activated receptor gamma (PPARγ), a ligand-activated transcription factor belonging to the nuclear receptor superfamily, is expressed in various tissues and cell types, such as white and brown adipose tissues, vascular smooth muscle cells, macrophages, and vascular endothelial cells (23). PPARγ is also widely present in the kidney, including PTs and collecting ducts (24). TZDs are well-known exogenous PPARγ agonists that exert pleiotropic effects, including an improvement of insulin sensitivity and anti-inflammatory effects (25). The use of TZDs has been limited because of important side effects such as edema and congestive heart failure (26, 27). TZD-induced volume expansion is largely because of an enhancement of renal sodium and water retention (28). In addition, TZDs stimulate

* For correspondence: Motonobu Nakamura, nakamura-stm@umin.ac.jp.

both NBCe1 and NHE3 activities through the PPARγ/proto-oncogene tyrosine-protein kinase Src/epidermal growth factor receptor/extracellular signal–regulated kinase (ERK)-dependent nongenomic signaling pathway in isolated rat, rabbit, and human PTs (22). On the other hand, a variety of endogenous PPARγ ligands such as oxidized low-density lipoproteins (LDLs), oxPLs, eicosanoids, and linoleate derivatives have also been identified (29, 30). 1-O-hexadecyl-2-azelaoyl-*sn*-glycero-3-phosphocholine (azPC), an oxidation product of LDL alkyl phosphatidylcholines (PCs) present in atherosclerotic lesions, is a potent PPARγ agonist (30). The binding affinity of azPC is almost equivalent to that of rosiglitazone (30). However, the influence of azPC on renal sodium and fluid transport remains unclear.

Therefore, in the present study, we used isolated PTs from rats, mice, and humans to investigate whether azPC affects renal PT sodium transport.

Results

Effects of azPC on NBCe1 activity in isolated rat PTs

To investigate the effects of azPC on PT transport, we first examined NBCe1 activity using freshly isolated and luminally collapsed PTs from rat kidneys. As shown in Figure 1*A* and Fig. S1, azPC rapidly stimulated NBCe1 activity in isolated rat PTs. The stimulatory effects of azPC on NBCe1 activity were dose dependent in the concentration range 0.04 to 0.3 μM, whereas no difference was observed between 0.3 μM azPC and 1.0 μM azPC. Therefore, we conducted further experiments using 0.3 μM azPC.

We next examined whether the stimulation of NBCe1 activity by azPC was dependent on PPARγ signaling using a specific PPARγ antagonist, GW9662 (2-chloro-5-nitro-*N*-phenylbenzamide; 5 μM). GW9662 completely inhibited the stimulatory effects of azPC on NBCe1 activity without affecting the basal NBCe1 activity (Fig. 1*B*). We also performed gene-silencing experiments with siRNA against PPARγ in cultured rat PTs, as previously described (20, 31). As shown in Figure 1*C*, 40 nM siRNA against PPARγ significantly suppressed the expression of PPARγ mRNA as compared with the scrambled negative control. In addition, treatment with 40 nM siRNA against PPARγ did not affect the basal NBCe1 activity as compared with the treatment with scrambled negative control, which completely blocked the stimulation of NBCe1 by azPC (Fig. 1*D*). Moreover, we examined the effect of azPC on NBCe1 protein expression in rat kidney cortex tissues using Western blot analysis. Figs. S2 and S3 show that azPC did not affect NBCe1 protein abundance. These results indicate that azPC stimulates NBCe1 activity *via* PPARγ-dependent signaling without altering NBCe1 protein expression.

Effects of azPC on luminal NHE activity in isolated rat PTs

Next, we focused on luminal NHE activity in freshly isolated rat PTs. Luminal NHE activity was measured using lumen-opened PTs, as previously described (22, 31–33). The

stimulatory effects of azPC on luminal NHE activity were observed in a dose-dependent manner (Figs. 2*A* and S5), similar to NBCe1 activity. Therefore, we used 0.3 μM azPC for subsequent experiments.

Next, we performed experiments using an NHE inhibitor, ethyl-isopropyl amiloride (EIPA; 100 μM). As shown in Figure 2*B*, the stimulatory effects of azPC were completely inhibited by EIPA. EIPA treatment partially, but significantly, decreased the basal activity by approximately 30% (Fig. 2*B*). NHEs are expressed on basolateral and luminal membranes of the PT (34, 35). NHE1, which is ubiquitously expressed on basolateral membranes, also plays an important role in Na^+–H^+ translocation in the PT (34). To confirm whether NHE1 contributes to the stimulatory effect of azPC on NHE activity, we examined the effect of a selective NHE1 inhibitor, cariporide (1 μM) on NHE activation by azPC. Figure 2*C* shows that cariporide did not affect the basal activity or azPC-induced stimulatory responses. These results suggest that azPC stimulates luminal NHE activity in rat PTs.

We next investigated whether the stimulation of luminal NHE activity by azPC was mediated by PPARγ using GW9662 (5 μM). GW9662 completely inhibited the stimulatory effects of azPC on luminal NHE activity without affecting the basal NHE activity (Fig. 2*D*). Furthermore, we performed gene-silencing experiments using siRNA against PPARγ at 40 nM. As shown in Figure 2*E*, siRNA treatment against PPARγ did not affect the basal NHE activity as compared with the treatment with scrambled negative control, which completely suppressed the stimulation of luminal NHE by azPC. Moreover, we examined the effect of azPC on NHE3 protein expression in rat kidney cortex tissues using Western blot analysis. Figs. S2 and S4 showed that azPC did not affect NHE3 protein abundance. Therefore, these results indicate that azPC stimulates luminal NHE activity *via* PPARγ-dependent signaling without altering NHE3 protein expression.

Signaling pathway for stimulation of NBCe1 and NHE activities by azPC in rats

We previously reported that TZDs stimulate PT sodium transport through the PPARγ/Src/epidermal growth factor receptor/ERK pathway (22). In this study, we confirmed whether the signaling mechanism of azPC-induced PT transport stimulation overlaps with that of TZD-induced PT transport stimulation. We examined the effect of a mitogen-activated protein/extracellular signal–regulated kinase kinase (MEK) inhibitor, PD98059 (2-(2-amino-3methoxyphenyl)chromone; 10 μM), on azPC-induced stimulation of PT transport by measuring NBCe1 and luminal NHE activities in freshly isolated rat PTs, and we analyzed the impact of azPC on ERK phosphorylation in rat kidney cortex tissues using Western blot analysis. As shown in Figure 3, *A* and *B*, PD98059 did not affect the basal activities of NBCe1 and NHE, and it completely inhibited the stimulatory effects of azPC on both NBCe1 and NHE activities. Western blot analysis revealed that azPC induced ERK phosphorylation in a dose-dependent manner (Figs. S6 and S7). Furthermore, azPC-induced ERK
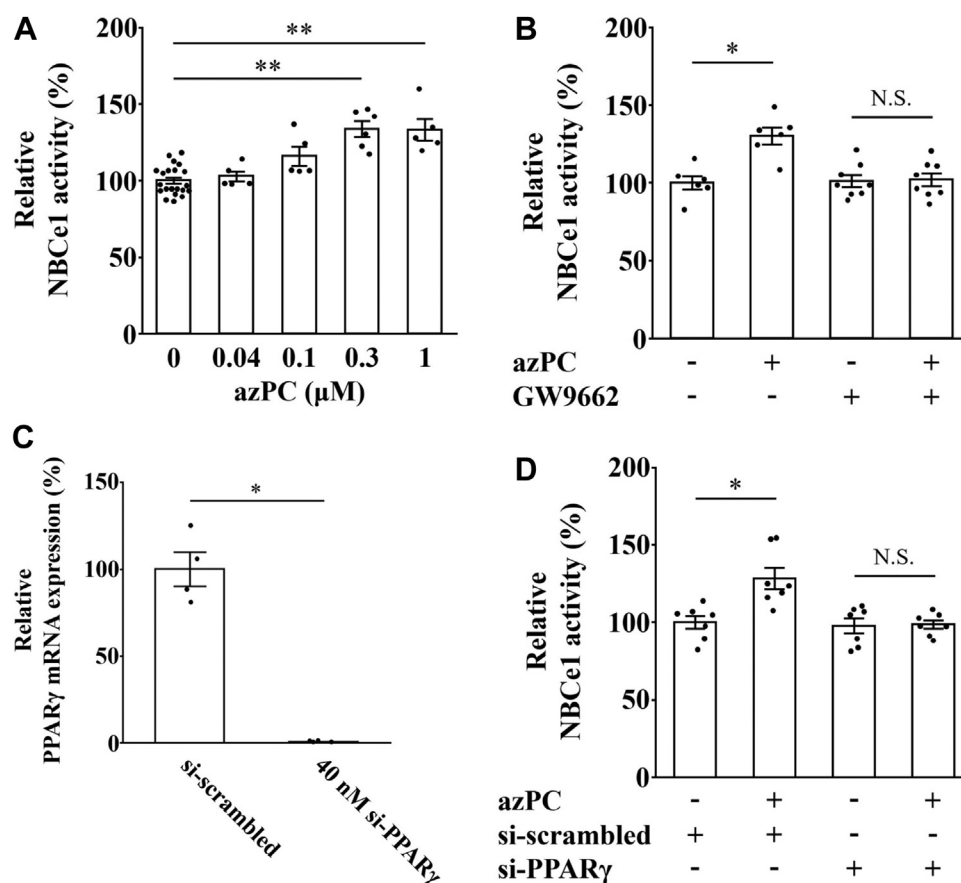
Figure 1. Effects of 1-O-hexadecyl-2-azelaoyl-*sn*-glycero-3-phosphocholine (azPC) on Na$^+$/HCO$_3^-$ cotransporter 1 (NBCe1) activity in rat proximal tubules (PTs). *A*, effects of azPC in the concentration range from 0.04 to 1 μM on NBCe1 activity in isolated rat PTs. Control, n = 21; 0.04 μM azPC, n = 5; 0.1 μM azPC, n = 5; 0.3 μM azPC, n = 6; 1 μM azPC, n = 5; **p < 0.01 *versus* control. *B*, effects of 5 μM GW9662 (2-chloro-5-nitro-*N*-phenylbenzamide) on NBCe1 activity in PTs treated with 0.3 μM azPC. Control, n = 6; azPC, n = 6; GW9662, n = 8; azPC + GW9662, n = 8; *p < 0.05 *versus* control. *C*, peroxisome proliferator–activated receptor gamma (PPARγ) mRNA expression in isolated rat PTs treated with siRNA against PPARγ at 40 nM (si-PPARγ) as compared with that in isolated rat PTs treated with scrambled negative control (si-scrambled). n = 4; *p < 0.05 *versus* si-scrambled. *D*, effects of siRNA treatment on 0.3 μM azPC-stimulated NBCe1 activity in isolated rat PTs. PTs were treated with si-scrambled or si-PPARγ. n = 7; *p < 0.05 *versus* si-scrambled. Each *open bar* represents the relative activity of NBCe1. NBCe1 activity of control group (azPC-untreated PT) was set at 100%.

phosphorylation was completely blocked by GW9662 and PD98059 (Fig. 3, *C–F*). These results suggest that azPC-induced stimulation of PT transport is dependent on the PPARγ/MEK/ERK signaling pathway.

The role of cluster determinant 36 in azPC-induced stimulation of PT transport in isolated rat PTs

It has been reported that cluster determinant 36 (CD36), a multifunctional receptor mediating the cellular uptake of various oxidation products, promotes the uptake of extracellular azPC in human monocytes (30). To confirm whether the stimulatory effects of azPC on PT transport were mediated by CD36, we examined the effect of a CD36 inhibitor, sulfosuccinimidyl oleate (SSO) (200 μM), on azPC-induced stimulation of PT transport by measuring NBCe1 and luminal NHE activities in cultured rat PTs. As shown in Figure 4, *A* and *B*, SSO completely inhibited the stimulatory effects of azPC on both NBCe1 and NHE activities without affecting the basal activities of NBCe1 and NHE. These results indicate that the azPC-induced stimulation of PT transport is mediated by CD36.

Acute in vivo *effect of azPC on renal sodium reabsorption*

We next examined whether azPC promoted renal sodium reabsorption in rats. We used rats fed a high-salt diet (8% NaCl) to detect rapid changes in renal sodium handling. Figure 5, *A–C* shows that azPC significantly reduced fractional excretion of sodium (FENa) without affecting creatinine clearance or urine volume. In addition, GW9662 administration completely blocked FENa reduction by azPC (Fig. 5*A*). Furthermore, we analyzed the effect of azPC on NBCe1 and NHE3 protein expression in rat kidney cortex tissues. As shown in Figure 5, *D–F*, we found no changes in protein abundances of NBCe1 and NHE3, similar to the *in vitro* experiments (Figs. S2–S4). These results indicate that azPC promotes renal sodium reabsorption through a PPARγ-dependent mechanism without altering the protein expression of NBCe1 and NHE3.

Effects of azPC on PT transport in humans

Next, we examined the effect of azPC on PT transport in humans. No patient showed a severe renal dysfunction (Table S1). Addition of 0.3 μM azPC stimulated both NBCe1
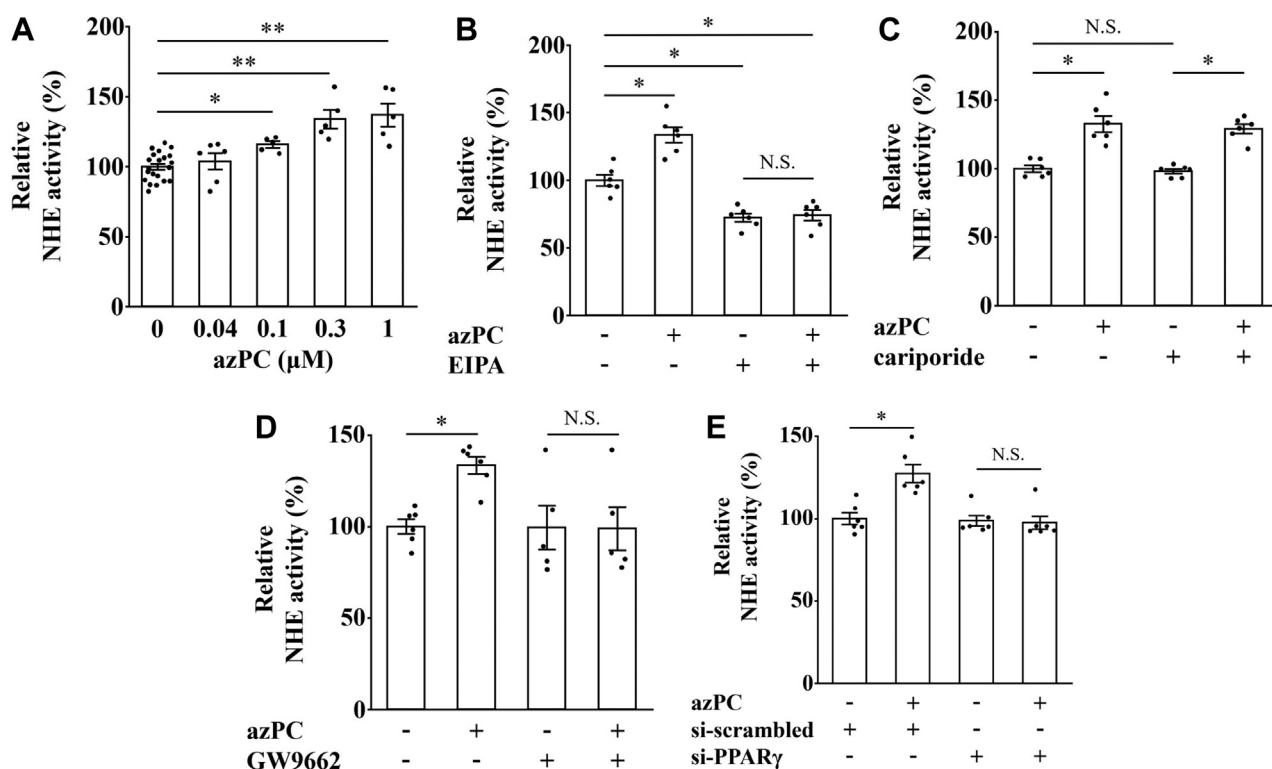
Figure 2. Effects of 1-O-hexadecyl-2-azelaoyl-*sn*-glycero-3-phosphocholine (azPC) on luminal Na⁺/H⁺ exchanger (NHE) activity in rat proximal tubules (PTs). *A*, effects of azPC in the concentration range from 0.04 to 1 μM on luminal NHE activity in isolated rat PTs. Control, n = 21; 0.04 μM azPC, n = 6; 0.1 μM azPC, n = 5; 0.3 μM azPC, n = 5; 1 μM azPC, n = 5; *$p < 0.05$, **$p < 0.01$ *versus* control. *B*, effects of 100 μM ethyl-isopropyl amiloride on luminal NHE activity in PTs treated with 0.3 μM azPC. n = 6; *$p < 0.05$ *versus* control. *C*, effects of 1 μM cariporide on luminal NHE activity in PTs treated with 0.3 μM azPC. n = 6; *$p < 0.05$ *versus* control. *D*, effects of 5 μM GW9662 (2-chloro-5-nitro-*N*-phenylbenzamide) on luminal NHE activity in PTs treated with 0.3 μM azPC. Control, n = 6; azPC, n = 6; GW9662, n = 5; azPC + GW9662, n = 5; *$p < 0.05$ *versus* control. *E*, effects of siRNA treatment on 0.3 μM azPC-stimulated luminal NHE activity in isolated rat PTs. PTs were treated with si-scrambled or siRNA against peroxisome proliferator–activated receptor gamma (PPARγ) at 40 nM. n = 6; *$p < 0.05$ *versus* si-scrambled. Each PT was also treated with 200 nM bafilomycin A₁. Each *open bar* represents the relative activity of luminal NHEs. NHE activity of the control group (azPC-untreated PT) was set at 100%.

and luminal NHE activities in freshly isolated human PTs, and the stimulatory responses were completely suppressed by GW9662 (Fig. 6, *A* and *B*). Moreover, Western blot analysis in human kidney cortex tissues revealed that 0.3 μM azPC significantly enhanced ERK phosphorylation, and the enhancement of ERK phosphorylation was completely blocked by GW9662 (Fig. 6, *C* and *D*). Thus, we observed that azPC stimulated human PT transport through the PPARγ/MEK/ERK signaling pathway as well as rat PT transport.

Discussion

In this study, we demonstrated that azPC rapidly stimulated renal PT sodium transport by activating both NBCe1 and luminal NHEs in rats and humans, and the stimulatory responses were mediated by PPARγ. The azPC-induced activation of NBCe1 and NHE was inhibited by PD98059 and SSO in isolated rat PTs. In addition, azPC enhanced ERK phosphorylation in kidney cortex tissues, and azPC-induced ERK phosphorylation was inhibited by GW9662 and PD98059. These results suggest that azPC stimulates sodium reabsorption from rat and human PTs through the PPARγ/MEK/ERK signaling pathway mediated by CD36 (Fig. 7).

The action of TZDs on sodium transporters in PT has been reported previously (36–38). For example, troglitazone has been reported to activate NBCe1 activity in rabbit PTs (36). Other studies have also reported that TZDs enhance the expression of NHE3 in human PT cells and rat kidneys (37, 38). However, the effect of endogenous PPARγ ligands on sodium transporters in PT is unknown. In this study, we demonstrated that 0.3 μM azPC stimulated NBCe1 activity by approximately 34 ± 5% in isolated rat PTs, which was comparable to that of NBCe1 activation by TZDs (approximately 35–40%) in our previous study using rat PTs (22). Several previous findings that the efficacy of other NBCe1 stimulants such as Ang II was approximately 25 to 60% also suggest that azPC has a sufficient impact on NBCe1 activity (18–20). Therefore, the effect of azPC on PT transport seems likely to be involved in volume expansion, although the effect of azPC on other nephrons, including collecting ducts, needs to be elucidated.

Nuclear receptors, including PPARγ, have been reported to exert rapid actions through a nongenomic mechanism in addition to the classical genomic mechanisms that regulate the transcription of target genes (39). The nongenomic actions of PPARγ can occur both in a PPARγ-dependent and PPARγ-independent manner (40, 41). Accumulating evidence suggests the involvement of the nongenomic actions of PPARγ in various physiological mechanisms such as platelet activation (42, 43), anti-inflammatory effects (44), antineoplastic effects
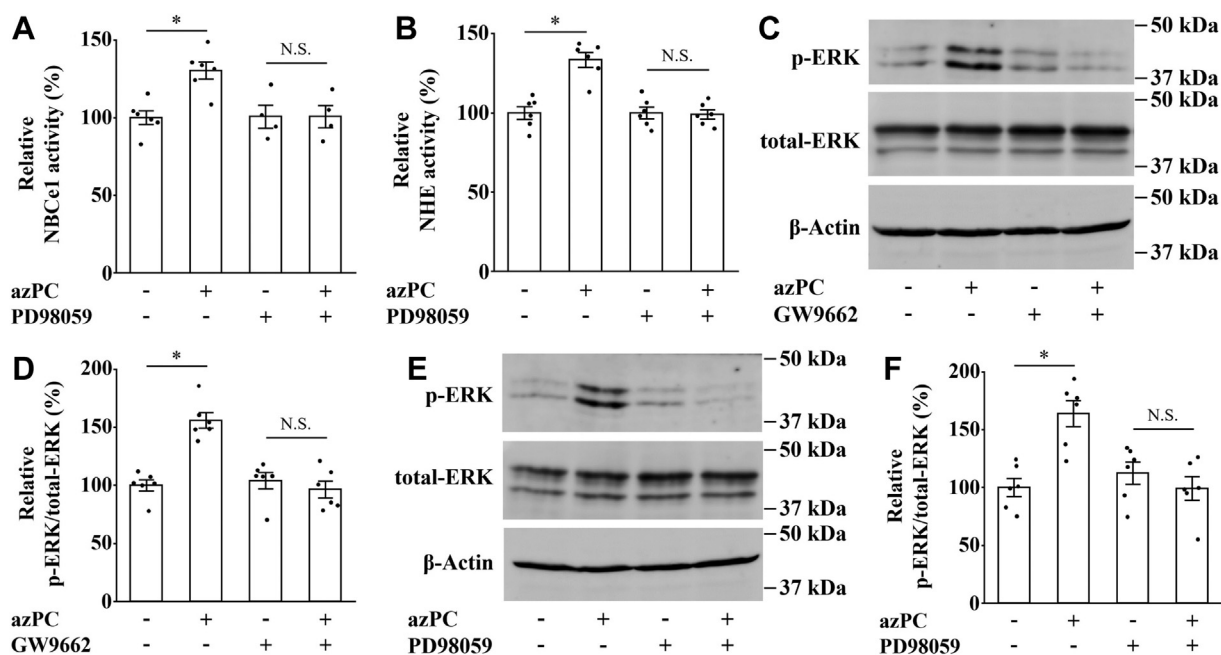
Figure 3. Role of extracellular signal–regulated kinase (ERK) in 1-O-hexadecyl-2-azelaoyl-*sn*-glycero-3-phosphocholine (azPC)-induced peroxisome proliferator–activated receptor gamma (PPARγ)-dependent pathway in ratproximal tubules (PTs). *A*, effects of 10 μM PD98059 (2-(2-amino-3methoxyphenyl)chromone) on Na^+/HCO_3^- cotransporter 1 (NBCe1) activity in PTs treated with 0.3 μM azPC. Control, n = 6; azPC, n = 6; PD98059, n = 4; azPC + PD98059, n = 4; *p < 0.05 versus* control. *B*, effects of 10 μM PD98059 on luminal Na^+/H^+ exchanger (NHE) activity in PTs treated with 0.3 μM azPC. n = 6; *p < 0.05 versus* control. *C*, ERK phosphorylation in rat kidney cortex tissues. Kidney samples were treated with 0.3 μM azPC in the presence or the absence of 5 μM GW9662 (2-chloro-5-nitro-*N*-phenylbenzamide). *D*, effects of 5 μM GW9662 on azPC-induced phosphorylation of ERK in rat kidney cortex tissues. n = 6; *p < 0.05 versus* azPC-untreated and GW9662-untreated kidney cortex. *E*, ERK phosphorylation in rat kidney cortex tissues. Kidney samples were treated with 0.3 μM azPC in the presence or the absence of 10 μM PD98059. *F*, effects of 10 μM PD98059 on azPC-induced phosphorylation of ERK in rat kidney cortex tissues. n = 6; *p < 0.05 versus* azPC-untreated and PD98059-untreated kidney cortex.

(45, 46), and neuropathic pain control (41); however, its role in renal transport is far from being elucidated. We previously demonstrated the nongenomic action of TZDs on PT sodium transport using mouse embryonic fibroblast cells from $PPAR\gamma^{-/-}$ mouse (22). This previous study showed that the rapid stimulation of NHE1 activity and ERK phosphorylation by TZDs depend on the ligand-binding ability but not the transcriptional activity of PPARγ (22). The short time frame in the range of seconds to minutes is essential to distinguish between nongenomic and genomic actions (39). The azPC-induced actions on PTs were exerted rapidly within a few

minutes, which were consistent with the features of non-genomic actions. In addition, azPC stimulated both NBCe1 and NHE3 activities without altering these protein abundances (Figs. S2–S4), which was consistent with previous studies showing that rapid nongenomic actions of steroid hormones do not increase in protein levels (47, 48). Furthermore, we found that azPC activated luminal NHEs in rat and human PTs but not in mouse PTs (Fig. S8), which was similar to TZD-induced actions (22). Therefore, these findings suggest that the PPARγ-dependent signaling pathway activated by azPC may overlap with the nongenomic signaling pathway activated
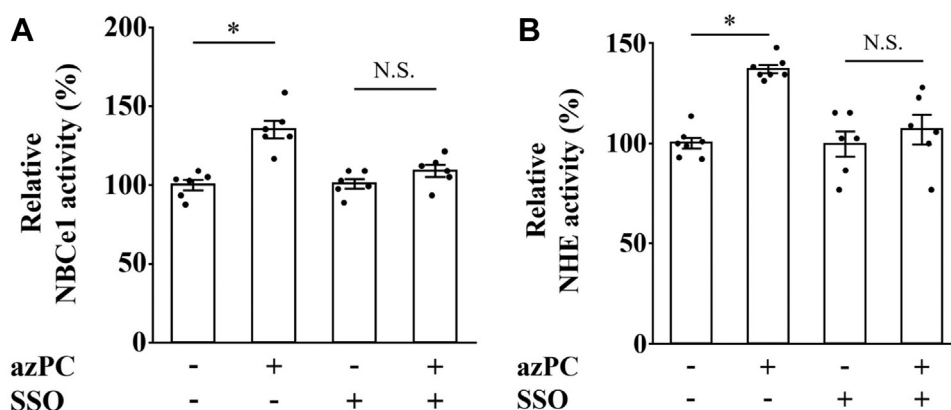
Figure 4. Effects of sulfosuccinimidyl oleate (SSO) on 1-O-hexadecyl-2-azelaoyl-*sn*-glycero-3-phosphocholine (azPC)-induced activation of Na^+/HCO_3^- cotransporter 1 (NBCe1) and Na^+/H^+ exchanger (NHE) in cultured rat proximal tubules (PTs). *A*, effects of 200 μM SSO on NBCe1 activity in PTs treated with 0.3 μM azPC. n = 6; *p < 0.05 versus* control. *B*, effects of 200 μM SSO on luminal NHE activity in PTs treated with 0.3 μM azPC. Control, n = 7; azPC, n = 7; SSO, n = 6; azPC + SSO, n = 6; *p < 0.05 versus* control.
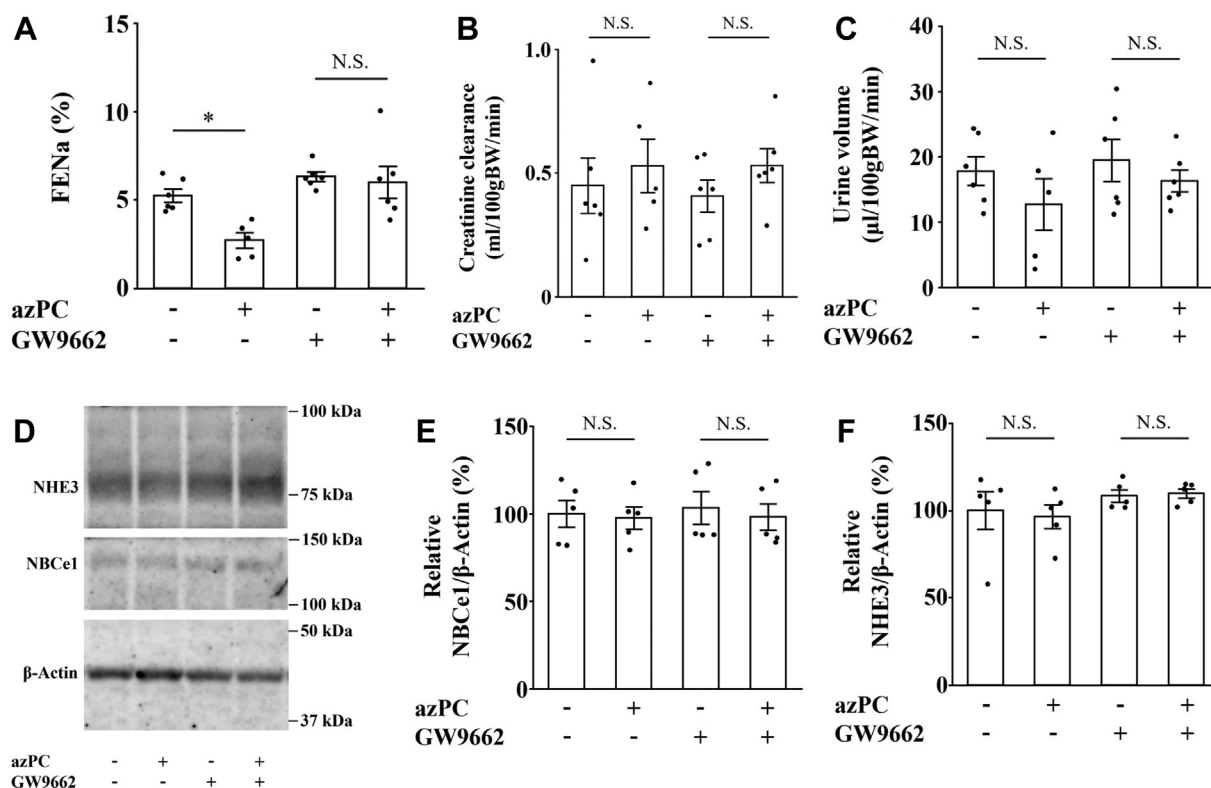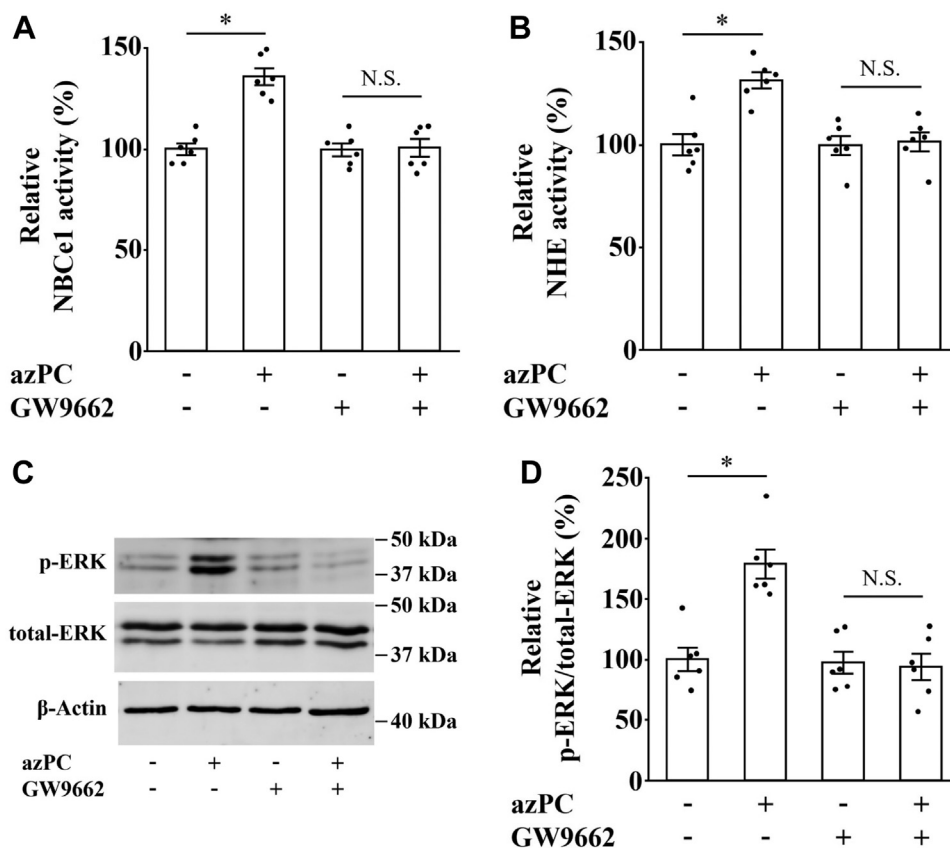
Figure 5. Effects of 1-O-hexadecyl-2-azelaoyl-*sn*-glycero-3-phosphocholine (azPC) on *in vivo* renal sodium and fluid transport in rats fed a high-salt diet (8% NaCl). Effects of azPC or GW9662 (2-chloro-5-nitro-*N*-phenylbenzamide) on fractional excretion of sodium (FENa; *A*), creatinine clearance (*B*), and urine volume (*C*) in acute renal clearance study. Control, n = 6; azPC, n = 5; GW9662, n = 6; azPC + GW9662, n = 6; *p < 0.05 *versus* control. *D*, Na$^+$/HCO$_3^-$ cotransporter 1 (NBCe1) and Na$^+$/H$^+$ exchanger (NHE3) protein expression in rat kidney cortex tissues. Kidney samples were collected 90 min after vehicle (control) or azPC administration. *E*, effects of azPC on NBCe1 protein expression in rat kidney cortex tissues. n = 5. *F*, effects of azPC on NHE3 protein expression in rat kidney cortex tissues. n = 5.

by TZDs. Although a variety of nongenomic signaling activated by PPARγ ligands has been described (49), the MEK/ERK pathway probably plays an important role in PT transport because multiple ligands such as TZDs and Ang II have been reported to activate both NBCe1 and NHE3 through the MEK/ERK pathway (19, 22).

We measured NHE activity by calculating the rate of decrease of intracellular pH (pH$_i$) caused by bath Na$^+$ removal and buffer capacity using lumen-opened PTs (31). To confirm the activation of NHE by azPC, we demonstrated that azPC-induced stimulation was completely inhibited by 100 μM EIPA (Fig. 2*B*). Furthermore, EIPA decreased the basal activity by approximately 30% (Fig. 2*B*), which seemed less effective than other studies because several previous studies have reported that EIPA reduces HCO$_3^-$ reabsorption in PTs by 40 to 60% using a microperfusion technique (32, 50, 51). Our results are presumed to be affected by sodium-coupled transporters other than luminal NHEs. Several studies have suggested the involvement of transporters other than NHE3 and V-ATPase in luminal sodium-coupled bicarbonate absorption in PTs (32, 50–52). The presence of a novel NBC on the luminal membranes of PTs has also been proposed in a recent study (53). Sodium-coupled transporters expressed on the luminal membranes of PTs can be reflected in our method while the function of NBCe1 is not significantly affected by Na$^+$

concentration (54). Cariporide was used to confirm whether azPC activated NHE1 expressed on the basolateral membranes of PTs (Fig. 2*C*) (35). The results showed that cariporide did not affect NHE activation by azPC, indicating that azPC activated luminal NHEs. Moreover, comparative studies using a microperfusion technique showed that the contribution of NHE2 to Na$^+$–H$^+$ translocation in PTs was less than that of NHE3 (50, 55). Based on these results, we determined that azPC can activate NHE3.

The stimulatory effects of azPC on PT sodium transport were dose dependent at submicromolar concentrations. The pharmacokinetics of azPC have not been fully understood, and the physiological concentration of azPC in PT is unknown. However, the concentrations of azPC used in the present study should be reasonable. It has been demonstrated that azPC dose-dependently induces PPAR response element reporter gene expression at submicromolar concentrations in CV-1 cells transfected with acyl-CoA-oxidase–PPAR response element–luciferase reporter plasmid (30). Other studies have also reported that 1 μM azPC exhibits sufficient PPARγ activation comparable to that of TZDs (56, 57). In addition, the plasma of humans and rodents contains low micromolar levels of total oxidatively fragmented PCs, and the plasma concentrations of several types of fragmented PCs such as 1-palmitoyl-2-(5-oxovaleroyl)-*sn*-glycero-3-phosphocholine are in low micromolar or submicromolar ranges. Thus, previous

Figure 6. Peroxisome proliferator–activated receptor gamma (PPARγ)-dependent stimulation of Na$^+$/HCO$_3^-$ cotransporter 1 (NBCe1) and luminal Na$^+$/H$^+$ exchanger (NHE) activities by 1-O-hexadecyl-2-azelaoyl-*sn*-glycero-3-phosphocholine (azPC) in humans. *A*, effects of 5 μM GW9662 (2-chloro-5-nitro-*N*-phenylbenzamide) on NBCe1 activity in human proximal tubules (PTs) treated with 0.3 μM azPC. n = 6; *$p < 0.05$ *versus* control. *B*, effects of 5 μM GW9662 on luminal NHE activity in human PTs treated with 0.3 μM azPC. n = 6; *$p < 0.05$ *versus* control. *C*, extracellular signal–regulated kinase (ERK) phosphorylation in human kidney cortex tissues. Kidney samples were treated with 0.3 μM azPC in the presence or the absence of 5 μM GW9662. *D*, effects of 5 μM GW9662 on azPC-induced phosphorylation of ERK in human kidney cortex tissues. n = 6; *$p < 0.05$ *versus* azPC-untreated and GW9662-untreated kidney cortex.

studies likely support the validity of the concentrations of azPC in the present study (7, 11, 58).

CD36, which mediates the cellular uptake of various oxidation products such as oxPLs and oxidized LDL, is
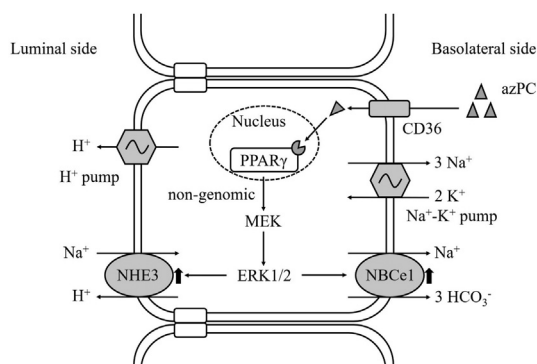
Figure 7. Schematic representation of the effect of 1-O-hexadecyl-2-azelaoyl-*sn*-glycero-3-phosphocholine (azPC) on sodium transport in proximal tubules (PTs). azPC activates basolateral Na$^+$/HCO$_3^-$ cotransporter 1 (NBCe1) and luminal Na$^+$/H$^+$ exchanger 3 (NHE3) through the peroxisome proliferator–activated receptor gamma (PPARγ)/mitogen-activated protein/extracellular signal–regulated kinase kinase (MEK)/extracellular signal–regulated kinase (ERK) signaling pathway, leading to the stimulation of sodium transport in PTs.

widely expressed in the PTs of the kidney (59). Although a previous study has reported that azPC enhances CD36 expression and that CD36 promotes the uptake of extracellular azPC in human monocytes (30), the association between azPC and CD36 in PT transport remains unclear. The present study demonstrated that azPC-induced PT transport stimulation was mediated by CD36 using SSO in isolated rat PTs. Previous findings that the downstream signaling triggered by renal CD36 includes the MEK/ERK pathway suggest that the PPARγ/MEK/ERK signaling activated by azPC is one of the downstream signals triggered by CD36 in the PT (60, 61).

In summary, we demonstrated that azPC rapidly activated basolateral NBCe1 and luminal NHEs *via* the PPARγ/MEK/ERK pathway mediated by CD36 in isolated PTs from rat and human kidneys. The stimulation of PT sodium and water reabsorption by azPC is likely a novel mechanism leading to the development of volume expansion. We believe that these findings can provide an impetus for elucidating the mechanism of atherosclerosis-induced volume expansion and hypertension because azPC is strongly associated with the development and progression of atherosclerosis.

Experimental procedures

Animal studies

Male Wistar rats and male C57BL/6 mice were purchased from CLEA Japan, Inc. They were housed in cages with a 12/12 h light/dark cycle, and they were provided a normal diet containing 0.5% NaCl (MF; Oriental Yeast Co, Ltd) and water ad libitum. Rats and mice, at 4 to 6 weeks of age, were sacrificed after anesthetization with excessive amounts of pentobarbital sodium (Somnopentyl) (intraperitoneally, 50 mg/kg), and the samples were obtained. All animal experiments were performed in accordance with local institutional guidelines (authorization number: P17-070).

Human samples

Human kidney samples were obtained from patients who underwent unilateral nephrectomy for renal carcinoma. The study was approved by the Institutional Review Board of the University of Tokyo School of Medicine (2520-[11]), and signed informed consent was obtained from all subjects. This study was conducted according to the principles expressed in the Declaration of Helsinki.

Measurements of NBCe1 activity in renal PTs from rats and humans

NBCe1 activity was determined as previously described (18, 22, 62). Briefly, the PT (S2 segment) fragment was manually microdissected from rat or human kidneys without collagenase treatment, and it was transferred to a perfusion chamber mounted on an inverted microscope. To avoid the influence of luminal transporters, the PT fragment was collapsed with two holding pipettes. The luminally collapsed PT was incubated with an acetoxymethyl ester form of a pH-sensitive fluorescent dye 2′,7′-bis(carboxyethyl)-5(6)-carboxyfluorescein acetoxymethyl ester (Dojindo Laboratories) in Dulbecco's modified Eagle's medium (DMEM) for 10 min, and pH_i was monitored with a photometry system, MetaFluor 7.7 software (Molecular Devices). The chamber was perfused with prewarmed (38 °C) DMEM equilibrated with 5% CO_2/95% O_2 gas, and subsequently, bath HCO_3^- concentrations were repeatedly switched from 25 to 12.5 mM in the absence and presence of azPC (Cayman Chemical Company) or other chemical agents such as a specific PPARγ antagonist GW9662 (Sigma–Aldrich) at 5 µM and an MEK inhibitor PD98059 (FUJIFILM Wako Pure Chemical) at 10 µM, both of which exhibit sufficient inhibitory activities without affecting the basal NBCe1 activity in PTs (19, 22). NBCe1 activity was calculated using the rate of pH_i decrease in response to bath HCO_3^- reduction and buffer capacity.

Measurements of luminal NHE activity in renal PTs from rats, mice, and humans

Luminal NHE activity was determined as previously described (22, 31, 33). Briefly, the PT (S2 segment) fragment was freshly isolated in the same way as the measurements of NBCe1 activity, and they were attached to a glass coverslip with Cell-tak glue (Corning). The tubule was placed on a perfusion chamber mounted on an inverted microscope, and the end of the tubule was cut with a capillary glass to sufficiently expose the lumen of the tubule. The lumen-opened PT was incubated with 2′,7′-bis(carboxyethyl)-5(6)-carboxyfluorescein acetoxymethyl ester in Hepes-buffered solution (144 mM Na^+, 5 mM K^+, 1.5 mM Ca^{2+}, 1 mM Mg^{2+}, 137 mM Cl^-, 2 mM $H_2PO_4^-$, 1 mM SO_4^{2-}, 5.5 mM glucose, 25 mM Hepes, adjusted to pH 7.4) (31, 63) for 10 min, and pH_i was monitored with MetaFluor 7.7 software. A prewarmed (38 °C) Hepes-buffered solution was used for the bath perfusate, and 200 nM bafilomycin A_1 (FUJIFILM Wako Pure Chemical) was added to block the effect of V-ATPase on PT transport (31, 33). The perfusate was repeatedly switched from Hepes-buffered solution to an isotonic Na^+-free solution (144 mM *N*-methyl-D-glucamine, 5 mM K^+, 1.5 mM Ca^{2+}, 1 mM Mg^{2+}, 137 mM Cl^-, 2 mM $H_2PO_4^-$, 1 mM SO_4^{2-}, 5.5 mM glucose, 25 mM Hepes, adjusted to pH 7.4) in the absence and presence of azPC or other chemical agents such as two NHE inhibitors EIPA (Research Biochemicals Incorporated) at 100 µM and cariporide (Santa Cruz Biotechnology) at 1 µM and GW9662 at 5 µM and PD98059 at 10 µM. EIPA was used at a concentration that significantly inhibited all isoforms of NHE (32, 64). Cariporide was used at a concentration that significantly inhibited NHE1 but not NHE3 in murine cells (64–66). GW9662 (5 µM) and PD98059 (10 µM) exhibited sufficient inhibitory activities without affecting the basal NHE activity in PTs (19, 22). Luminal NHE activity was calculated using the rate of pH_i decrease caused by bath Na^+ removal and buffer capacity.

siRNA treatment in isolated rat PTs

siRNA treatment of isolated rat PTs was performed as previously described (20, 31). Briefly, freshly isolated rat PTs were treated with siRNA against PPARγ (AM16708; Invitrogen) at 40 nM or scrambled negative control (sc-37007; Santa Cruz Biotechnology) using Lipofectamine 2000 and Opti-MEM I Reduced Serum Medium (both from Invitrogen). The PTs were incubated in DMEM supplemented with 10% fetal bovine serum at 37 °C overnight, and they were used to measure NBCe1 activity, luminal NHE activity, and quantitative PCR.

RNA extraction and quantitative PCR analysis

Total RNA was extracted from isolated rat PTs with isogen II (Nippon Gene), according to the manufacturer's instructions, and first-strand complementary DNA was synthesized using a cDNA Synthesis Kit (Takara), as previously reported (20). The mRNA expression levels were estimated using quantitative PCR (Prism 7000; Applied Biosystems) with TaqMan Gene Expression Master Mix (Applied Biosystems) and TaqMan Gene Expression Assay kits, Rn00440945_m1 for rat PPARγ, Rn00580728_m1 for rat CD36, or Rn00667869_m1 for rat β-actin (Applied Biosystems). The mRNA levels were normalized to β-actin expression levels.

Western blot analysis

Thin slices of kidney cortex were obtained from rats or humans, and they were divided into small bundles, as previously described (22, 67). The kidney samples were incubated in DMEM at 37 °C under 5% CO_2 for 40 min in the presence or the absence of inhibitors such as 5 µM GW9662 and 10 µM PD98059, and they were incubated for 15 min in DMEM containing 0.3 µM azPC. After incubation, the samples were homogenized in ice-cold buffer A (25 mM Tris–HCl [pH 7.4], 10 mM sodium orthovanadate, 10 mM sodium pyrophosphate, 100 mM sodium fluoride, 10 mM EDTA, 10 mM EGTA, and 1 mM phenylmethylsulfonyl fluoride) (22), and they were centrifuged at 12,000*g* for 10 min. The supernatant from each sample was collected and divided into aliquots containing equal amounts (approximately 20 µg) of proteins. The samples were separated using 10% SDS-PAGE, and they were transferred onto nitrocellulose membranes. After the membranes were blocked with 5% skim milk in Tris-buffered saline (137 mM NaCl, 2.68 mM KCl, 25 mM Tris, adjusted to pH 7.4), they were incubated with primary antibodies at 4 °C overnight, and following this, they were incubated with horseradish peroxidase (HRP)–conjugated secondary antibodies at room temperature for 1 h. Primary antibodies against ERK1/2 (9102), phospho-ERK1/2 (Thr202/Tyr204) (9101), and β-actin (4970) were purchased from Cell Signaling Technology, and the primary antibodies against NBCe1 (sc-515543) and NHE3 (sc-136368) were purchased from Santa Cruz Biotechnology. HRP-conjugated anti-rabbit IgG antibody (111-035-003) and HRP-conjugated antimouse IgG antibody (115-035-003) were purchased from Jackson ImmunoResearch Laboratories. The protein bands were detected using a chemiluminescence detection system (ImageQuant LAS 4000 mini; GE Healthcare).

Treatment with SSO in isolated rat PTs

Freshly isolated rat PTs were incubated in DMEM supplemented with 10% fetal bovine serum and 200 µM SSO (Cayman Chemical Company) or an equal volume of dimethyl sulfoxide at 37 °C under 5% CO_2. After overnight incubation, they were used to measure NBCe1 activity and luminal NHE activity. SSO was used at a concentration that significantly inhibited the transport function of CD36 in various cell types (68, 69).

Rat *in vivo* experimental protocol

Male Wistar rats weighing 130 to 200 g were randomly assigned into four groups: ethanol/ethanol (control, n = 6), GW9662/ethanol (GW9662 only, n = 6), ethanol/azPC (azPC only, n = 5), and GW9662/azPC (n = 6). After an acclimation period, the diet was changed from a normal diet (0.5% NaCl) to a high-salt diet (8% NaCl) (F2Dahl-8.0; Oriental Yeast Co, Ltd) a week before the experiment. To facilitate the detection of rapid changes among groups, a high-salt diet was selected according to a previous report showing that high-salt diet increased FENa and urine volume (70). Rats were intraperitoneally administered with GW9662 (1 mg/kg) or an equal volume of ethanol (vehicle for GW9662) 24 and 12 h before the experiment (71). On the day of the experiment, 30 min after a load of tap water by gavage (10 ml/kg), rats were intraperitoneally administered with azPC (10 mg/kg; diluted with half saline) or an equal volume of ethanol diluted with half saline (vehicle for azPC, 10 ml/kg). Urine was collected for 90 min after azPC or ethanol injection in a metabolic cage. At the end of the experiment, rats were sacrificed after anesthetization with pentobarbital sodium, and blood and kidney samples were obtained. Blood and urine data were measured by SRL Clinical Laboratory Service. FENa and creatinine clearance were calculated using standard formulas. The amount of NBCe1 and NHE3 in the kidney cortex was determined using Western blot analysis.

Statistical analysis

All data are expressed as the mean ± standard error of the mean. The data were analyzed with JMP Pro 14 software (SAS Institute) using a Wilcoxon signed-rank test or Kruskal–Wallis test followed by a Steel test or Steel–Dwass test, as appropriate. Statistical significance was set at a *p* value <0.05.

Data availability

The data supporting the findings of this study are included within the article and its supporting information.

phospholipid; PC, phosphatidylcholine; PD98059, 2-(2-amino-3methoxyphenyl)chromone; pHi, intracellular pH; PPARγ, peroxisome proliferator–activated receptor gamma; PT, proximal tubule; SSO, sulfosuccinimidyl oleate; TZD, thiazolidinedione; V-ATPase, vacuolar-type H$^+$-ATPase.

References

1. Ziegler, T., Abdel Rahman, F., Jurisch, V., and Kupatt, C. (2019) Atherosclerosis and the capillary network; pathophysiology and potential therapeutic strategies. *Cells* **9**, 50
2. Pan, W. H., Bai, C. H., Chen, J. R., and Chiu, H. C. (1997) Associations between carotid atherosclerosis and high factor VIII activity, dyslipidemia, and hypertension. *Stroke* **28**, 88–94
3. Bochkov, V. N., Oskolkova, O. V., Birukov, K. G., Levonen, A. L., Binder, C. J., and Stöckl, J. (2010) Generation and biological activities of oxidized phospholipids. *Antioxid. Redox Signal.* **12**, 1009–1059
4. Yin, H., Xu, L., and Porter, N. A. (2011) Free radical lipid peroxidation: Mechanisms and analysis. *Chem. Rev.* **111**, 5944–5972
5. Lee, S., Birukov, K. G., Romanoski, C. E., Springstead, J. R., Lusis, A. J., and Berliner, J. A. (2012) Role of phospholipid oxidation products in atherosclerosis. *Circ. Res.* **111**, 778–799
6. Berliner, J. A., Leitinger, N., and Tsimikas, S. (2009) The role of oxidized phospholipids in atherosclerosis. *J. Lipid Res.* **50**, S207–S212
7. Greig, F. H., Kennedy, S., and Spickett, C. M. (2012) Physiological effects of oxidized phospholipids and their cellular signaling mechanisms in inflammation. *Free Radic. Biol. Med.* **52**, 266–280
8. Johnstone, S. R., Ross, J., Rizzo, M. J., Straub, A. C., Lampe, P. D., Leitinger, N., and Isakson, B. E. (2009) Oxidized phospholipid species promote *in vivo* differential cx43 phosphorylation and vascular smooth muscle cell proliferation. *Am. J. Pathol.* **175**, 916–924
9. Pidkovka, N. A., Cherepanova, O. A., Yoshida, T., Alexander, M. R., Deaton, R. A., Thomas, J. A., Leitinger, N., and Owens, G. K. (2007) Oxidized phospholipids induce phenotypic switching of vascular smooth muscle cells *in vivo* and *in vitro*. *Circ. Res.* **101**, 792–801
10. Cherepanova, O. A., Pidkovka, N. A., Sarmento, O. F., Yoshida, T., Gan, Q., Adiguzel, E., Bendeck, M. P., Berliner, J., Leitinger, N., and Owens, G. K. (2009) Oxidized phospholipids induce type VIII collagen expression and vascular smooth muscle cell migration. *Circ. Res.* **104**, 609–618
11. Oskolkova, O. V., Afonyushkin, T., Preinerstorfer, B., Bicker, W., von Schlieffen, E., Hainzl, E., Demyanets, S., Schabbauer, G., Lindner, W., Tselepis, A. D., Wojta, J., Binder, B. R., and Bochkov, V. N. (2010) Oxidized phospholipids are more potent antagonists of lipopolysaccharide than inducers of inflammation. *J. Immunol.* **185**, 7706–7712
12. Que, X., Hung, M. Y., Yeang, C., Gonen, A., Prohaska, T. A., Sun, X., Diehl, C., Määttä, A., Gaddis, D. E., Bowden, K., Pattison, J., MacDonald, J. G., Ylä-Herttuala, S., Mellon, P. L., Hedrick, C. C., *et al.* (2018) Oxidized phospholipids are proinflammatory and proatherogenic in hypercholesterolaemic mice. *Nature* **558**, 301–306
13. Li, X. C., and Zhuo, J. L. (2016) Recent updates on the proximal tubule renin-angiotensin system in angiotensin II-dependent hypertension. *Curr. Hypertens. Rep.* **18**, 63
14. Zhuo, J. L., and Li, X. C. (2013) Proximal nephron. *Compr. Physiol.* **3**, 1079–1123
15. Soi, V., and Yee, J. (2017) Sodium homeostasis in chronic kidney disease. *Adv. Chronic Kidney Dis.* **24**, 325–331
16. Kurtz, I. (2014) Molecular mechanisms and regulation of urinary acidification. *Compr. Physiol.* **4**, 1737–1774
17. Thornell, I. M., and Bevensee, M. O. (2015) Regulators of Slc4 bicarbonate transporter activity. *Front. Physiol.* **6**, 166
18. Li, Y., Yamada, H., Kita, Y., Kunimi, M., Horita, S., Suzuki, M., Endo, Y., Shimizu, T., Seki, G., and Fujita, T. (2008) Roles of ERK and cPLA2 in the angiotensin II-mediated biphasic regulation of Na+-HCO3(-) transport. *J. Am. Soc. Nephrol.* **19**, 252–259
19. Shirai, A., Yamazaki, O., Horita, S., Nakamura, M., Satoh, N., Yamada, H., Suzuki, M., Kudo, A., Kawakami, H., Hofmann, F., Nishiyama, A., Kume, H., Enomoto, Y., Homma, Y., and Seki, G. (2014) Angiotensin
20. Nakamura, M., Yamazaki, O., Shirai, A., Horita, S., Satoh, N., Suzuki, M., Hamasaki, Y., Noiri, E., Kume, H., Enomoto, Y., Homma, Y., and Seki, G. (2015) Preserved Na/HCO3 cotransporter sensitivity to insulin may promote hypertension in metabolic syndrome. *Kidney Int.* **87**, 535–542
21. Nakamura, M., Tsukada, H., Seki, G., Satoh, N., Mizuno, T., Fujii, W., Horita, S., Moriya, K., Sato, Y., Kume, H., Nangaku, M., and Suzuki, M. (2020) Insulin promotes sodium transport but suppresses gluconeogenesis via distinct cellular pathways in human and rat renal proximal tubules. *Kidney Int.* **97**, 316–326
22. Endo, Y., Suzuki, M., Yamada, H., Horita, S., Kunimi, M., Yamazaki, O., Shirai, A., Nakamura, M., Iso, O. N., Li, Y., Hara, M., Tsukamoto, K., Moriyama, N., Kudo, A., Kawakami, H., *et al.* (2011) Thiazolidinediones enhance sodium-coupled bicarbonate absorption from renal proximal tubules via PPARγ-dependent nongenomic signaling. *Cell Metab.* **13**, 550–561
23. Hsueh, W. A., Jackson, S., and Law, R. E. (2001) Control of vascular cell proliferation and migration by PPAR-gamma: A new approach to the macrovascular complications of diabetes. *Diabetes Care* **24**, 392–397
24. Sato, K., Sugawara, A., Kudo, M., Uruno, A., Ito, S., and Takeuchi, K. (2004) Expression of peroxisome proliferator-activated receptor isoform proteins in the rat kidney. *Hypertens. Res.* **27**, 417–425
25. Davidson, M. A., Mattison, D. R., Azoulay, L., and Krewski, D. (2018) Thiazolidinedione drugs in the treatment of type 2 diabetes mellitus: Past, present and future. *Crit. Rev. Toxicol.* **48**, 52–108
26. Lago, R. M., Singh, P. P., and Nesto, R. W. (2007) Congestive heart failure and cardiovascular death in patients with prediabetes and type 2 diabetes given thiazolidinediones: A meta-analysis of randomised clinical trials. *Lancet* **370**, 1129–1136
27. Komajda, M., McMurray, J. J., Beck-Nielsen, H., Gomis, R., Hanefeld, M., Pocock, S. J., Curtis, P. S., Jones, N. P., and Home, P. D. (2010) Heart failure events in type 2 diabetes: Data from the RECORD clinical trial. *Eur. Heart J.* **31**, 824–831
28. Horita, S., Nakamura, M., Satoh, N., Suzuki, M., and Seki, G. (2015) Thiazolidinediones and edema: Recent advances in the pathogenesis of thiazolidinediones-induced renal sodium retention. *PPAR Res.* **2015**, 646423
29. Marion-Letellier, R., Savoye, G., and Ghosh, S. (2016) Fatty acids, eicosanoids and PPAR gamma. *Eur. J. Pharmacol.* **785**, 44–49
30. Davies, S. S., Pontsler, A. V., Marathe, G. K., Harrison, K. A., Murphy, R. C., Hinshaw, J. C., Prestwich, G. D., Hilaire, A. S., Prescott, S. M., Zimmerman, G. A., and McIntyre, T. M. (2001) Oxidized alkyl phospholipids are specific, high affinity peroxisome proliferator-activated receptor gamma ligands and agonists. *J. Biol. Chem.* **276**, 16015–16023
31. Satoh, N., Yamada, H., Yamazaki, O., Suzuki, M., Nakamura, M., Suzuki, A., Ashida, A., Yamamoto, D., Kaku, Y., Sekine, T., Seki, G., and Horita, S. (2016) A pure chloride channel mutant of CLC-5 causes Dent's disease via insufficient V-ATPase activation. *Pflugers Arch.* **468**, 1183–1196
32. Wang, T., Yang, C. L., Abbiati, T., Schultheis, P. J., Shull, G. E., Giebisch, G., and Aronson, P. S. (1999) Mechanism of proximal tubule bicarbonate absorption in NHE3 null mice. *Am. J. Physiol.* **277**, F298–F302
33. Nakamura, M., Satoh, N., Tsukada, H., Mizuno, T., Fujii, W., Suzuki, A., Horita, S., Nangaku, M., and Suzuki, M. (2020) Stimulatory effect of insulin on H+-ATPase in the proximal tubule via the Akt/mTORC2 pathway. *Physiol Int.* **107**, 376–389
34. Parker, M. D., Myers, E. J., and Schelling, J. R. (2015) Na+-H+ exchanger-1 (NHE1) regulation in kidney proximal tubule. *Cell. Mol. Life Sci.* **72**, 2061–2074
35. Biemesderfer, D., Reilly, R. F., Exner, M., Igarashi, P., and Aronson, P. S. (1992) Immunocytochemical characterization of Na(+)-H+ exchanger isoform NHE-1 in rabbit kidney. *Am. J. Physiol.* **263**, F833–F840
36. Muto, S., Miyata, Y., Imai, M., and Asano, Y. (2001) Troglitazone stimulates basolateral rheogenic Na+/HCO3- cotransport activity in rabbit proximal straight tubules. *Exp. Nephrol.* **9**, 191–197
37. Saad, S., Agapiou, D. J., Chen, X. M., Stevens, V., and Pollock, C. A. (2009) The role of Sgk-1 in the upregulation of transport proteins by PPAR-

ASBMB

{gamma} agonists in human proximal tubule cells. *Nephrol. Dial. Transpl.* **24**, 1130–1141

38. Song, J., Knepper, M. A., Hu, X., Verbalis, J. G., and Ecelbarger, C. A. (2004) Rosiglitazone activates renal sodium- and water-reabsorptive pathways and lowers blood pressure in normal rats. *J. Pharmacol. Exp. Ther.* **308**, 426–433

39. Lösel, R., and Wehling, M. (2003) Nongenomic actions of steroid hormones. *Nat. Rev. Mol. Cell. Biol.* **4**, 46–56

40. Luconi, M., Cantini, G., and Serio, M. (2010) Peroxisome proliferator-activated receptor gamma (PPARgamma): Is the genomic activity the only answer? *Steroids* **75**, 585–594

41. Griggs, R. B., Donahue, R. R., Morgenweck, J., Grace, P. M., Sutton, A., Watkins, L. R., and Taylor, B. K. (2015) Pioglitazone rapidly reduces neuropathic pain through astrocyte and nongenomic PPARγ mechanisms. *Pain* **156**, 469–482

42. Moraes, L. A., Spyridon, M., Kaiser, W. J., Jones, C. I., Sage, T., Atherton, R. E., and Gibbins, J. M. (2010) Non-genomic effects of PPARgamma ligands: Inhibition of GPVI-stimulated platelet activation. *J. Thromb. Haemost.* **8**, 577–587

43. Chou, T. C. (2014) New mechanisms of antiplatelet activity of nifedipine, an L-type calcium channel blocker. *Biomedicine (Taipei)* **4**, 24

44. Cantini, G., Lombardi, A., Borgogni, E., Francalanci, M., Ceni, E., Degl'Innocenti, S., Gelmini, S., Poli, G., Galli, A., Serio, M., Forti, G., and Luconi, M. (2010) Peroxisome-proliferator-activated receptor gamma (PPARgamma) is required for modulating endothelial inflammatory response through a nongenomic mechanism. *Eur. J. Cell Biol.* **89**, 645–653

45. Papageorgiou, E., Pitulis, N., Msaouel, P., Lembessis, P., and Koutsilieris, M. (2007) The non-genomic crosstalk between PPAR-gamma ligands and ERK1/2 in cancer cell lines. *Expert Opin. Ther. Targets* **11**, 1071–1085

46. Papageorgiou, E., Pitulis, N., Manoussakis, M., Lembessis, P., and Koutsilieris, M. (2008) Rosiglitazone attenuates insulin-like growth factor 1 receptor survival signaling in PC-3 cells. *Mol. Med.* **14**, 403–411

47. Wang, D., Zhang, H., Lang, F., and Yun, C. C. (2007) Acute activation of NHE3 by dexamethasone correlates with activation of SGK1 and requires a functional glucocorticoid receptor. *Am. J. Physiol. Cell Physiol.* **292**, C396–C404

48. Prevoo, B., Miller, D. S., van de Water, F. M., Wever, K. E., Russel, F. G., Flik, G., and Masereeuw, R. (2011) Rapid, nongenomic stimulation of multidrug resistance protein 2 (Mrp2) activity by glucocorticoids in renal proximal tubule. *J. Pharmacol. Exp. Ther.* **338**, 362–371

49. Gardner, O. S., Dewar, B. J., and Graves, L. M. (2005) Activation of mitogen-activated protein kinases by peroxisome proliferator-activated receptor ligands: An example of nongenomic signaling. *Mol. Pharmacol.* **68**, 933–941

50. Wang, T., Hropot, M., Aronson, P. S., and Giebisch, G. (2001) Role of NHE isoforms in mediating bicarbonate reabsorption along the nephron. *Am. J. Physiol. Renal Physiol.* **281**, F1117–F1122

51. Bailey, M. A. (2004) Inhibition of bicarbonate reabsorption in the rat proximal tubule by activation of luminal P2Y1 receptors. *Am. J. Physiol. Renal Physiol.* **287**, F789–F796

52. Schultheis, P. J., Clarke, L. L., Meneton, P., Miller, M. L., Soleimani, M., Gawenis, L. R., Riddle, T. M., Duffy, J. J., Doetschman, T., Wang, T., Giebisch, G., Aronson, P. S., Lorenz, J. N., and Shull, G. E. (1998) Renal and intestinal absorptive defects in mice lacking the NHE3 Na+/H+ exchanger. *Nat. Genet.* **19**, 282–285

53. Guo, Y. M., Liu, Y., Liu, M., Wang, J. L., Xie, Z. D., Chen, K. J., Wang, D. K., Occhipinti, R., Boron, W. F., and Chen, L. M. (2017) Na(+)/HCO(3)(-) cotransporter NBCn2 mediates HCO(3)(-) reclamation in the apical membrane of renal proximal tubules. *J. Am. Soc. Nephrol.* **28**, 2409–2419

54. Lo, Y. F., Yang, S. S., Seki, G., Yamada, H., Horita, S., Yamazaki, O., Fujita, T., Usui, T., Tsai, J. D., Yu, I. S., Lin, S. W., and Lin, S. H. (2011) Severe metabolic acidosis causes early lethality in NBC1 W516X knock-in mice as a model of human isolated proximal renal tubular acidosis. *Kidney Int.* **79**, 730–741

55. Choi, J. Y., Shah, M., Lee, M. G., Schultheis, P. J., Shull, G. E., Muallem, S., and Baum, M. (2000) Novel amiloride-sensitive sodium-dependent proton secretion in the mouse proximal convoluted tubule. *J. Clin. Invest.* **105**, 1141–1146

56. Pontsler, A. V., St Hilaire, A., Marathe, G. K., Zimmerman, G. A., and McIntyre, T. M. (2002) Cyclooxygenase-2 is induced in monocytes by peroxisome proliferator activated receptor gamma and oxidized alkyl phospholipids from oxidized low density lipoprotein. *J. Biol. Chem.* **277**, 13029–13036

57. Zhang, Q., Southall, M. D., Mezsick, S. M., Johnson, C., Murphy, R. C., Konger, R. L., and Travers, J. B. (2005) Epidermal peroxisome proliferator-activated receptor gamma as a target for ultraviolet B radiation. *J. Biol. Chem.* **280**, 73–79

58. Frey, B., Haupt, R., Alms, S., Holzmann, G., König, T., Kern, H., Kox, W., Rüstow, B., and Schlame, M. (2000) Increase in fragmented phosphatidylcholine in blood plasma by oxidative stress. *J. Lipid Res.* **41**, 1145–1153

59. Yang, X., Okamura, D. M., Lu, X., Chen, Y., Moorhead, J., Varghese, Z., and Ruan, X. Z. (2017) CD36 in chronic kidney disease: Novel insights and therapeutic opportunities. *Nat. Rev. Nephrol.* **13**, 769–781

60. Gao, X., Wu, J., Qian, Y., Fu, L., Wu, G., Xu, C., and Mei, C. (2014) Oxidized high-density lipoprotein impairs the function of human renal proximal tubule epithelial cells through CD36. *Int. J. Mol. Med.* **34**, 564–572

61. Baranova, I. N., Bocharov, A. V., Vishnyakova, T. G., Kurlander, R., Chen, Z., Fu, D., Arias, I. M., Csako, G., Patterson, A. P., and Eggerman, T. L. (2010) CD36 is a novel serum amyloid A (SAA) receptor mediating SAA binding and SAA-induced signaling in human and rodent cells. *J. Biol. Chem.* **285**, 8492–8506

62. Horita, S., Zheng, Y., Hara, C., Yamada, H., Kunimi, M., Taniguchi, S., Uwatoko, S., Sugaya, T., Goto, A., Fujita, T., and Seki, G. (2002) Biphasic regulation of Na+-HCO3- cotransporter by angiotensin II type 1A receptor. *Hypertension* **40**, 707–712

63. Yamada, H., Seki, G., Taniguchi, S., Uwatoko, S., Nosaka, K., Suzuki, K., and Kurokawa, K. (1996) Roles of Ca2+ and PKC in regulation of acid/base transport in isolated proximal tubules. *Am. J. Physiol.* **271**, F1068–F1076

64. Masereel, B., Pochet, L., and Laeckmann, D. (2003) An overview of inhibitors of Na(+)/H(+) exchanger. *Eur. J. Med. Chem.* **38**, 547–554

65. Pinto, V., Pinho, M. J., Hopfer, U., Jose, P. A., and Soares-da-Silva, P. (2008) Oxidative stress and the genomic regulation of aldosterone-stimulated NHE1 activity in SHR renal proximal tubular cells. *Mol. Cell. Biochem.* **310**, 191–201

66. Bachmann, O., Riederer, B., Rossmann, H., Groos, S., Schultheis, P. J., Shull, G. E., Gregor, M., Manns, M. P., and Seidler, U. (2004) The Na+/H+ exchanger isoform 2 is the predominant NHE isoform in murine colonic crypts and its lack causes NHE3 upregulation. *Am. J. Physiol. Gastrointest. Liver Physiol.* **287**, G125–G133

67. Zheng, Y., Yamada, H., Sakamoto, K., Horita, S., Kunimi, M., Endo, Y., Li, Y., Tobe, K., Terauchi, Y., Kadowaki, T., Seki, G., and Fujita, T. (2005) Roles of insulin receptor substrates in insulin-induced stimulation of renal proximal bicarbonate absorption. *J. Am. Soc. Nephrol.* **16**, 2288–2295

68. Coort, S. L., Willems, J., Coumans, W. A., van der Vusse, G. J., Bonen, A., Glatz, J. F., and Luiken, J. J. (2002) Sulfo-N-succinimidyl esters of long chain fatty acids specifically inhibit fatty acid translocase (FAT/CD36)-mediated cellular fatty acid uptake. *Mol. Cell. Biochem.* **239**, 213–219

69. Hua, W., Huang, H. Z., Tan, L. T., Wan, J. M., Gui, H. B., Zhao, L., Ruan, X. Z., Chen, X. M., and Du, X. G. (2015) CD36 mediated fatty acid-induced podocyte apoptosis via oxidative stress. *PLoS One* **10**, e0127507

70. Morita, H., Kurihara, H., Kurihara, Y., Shindo, T., Kuwaki, T., Kumada, M., and Yazaki, Y. (1998) Systemic and renal response to salt loading in endothelin-1 knockout mice. *J. Cardiovasc. Pharmacol.* **31**, S557–S560

71. Collino, M., Patel, N. S., Lawrence, K. M., Collin, M., Latchman, D. S., Yaqoob, M. M., and Thiemermann, C. (2005) The selective PPARgamma antagonist GW9662 reverses the protection of LPS in a model of renal ischemia-reperfusion. *Kidney Int.* **68**, 529–536